JCTC Journal of Chemical Theory and Computation

Article

pubs.acs.org/JCTC

Barrier Heights in Quantum Monte Carlo with Linear-Scaling Generalized-Valence-Bond Wave Functions

Francesco Fracchia,*[,†] Claudia Filippi,*[,‡] and Claudio Amovilli*[,§]

[†]Dipartimento di Scienze Chimiche e Farmaceutiche, Università di Ferrara, Via L. Borsari 46, 44121 Ferrara, Italy

[‡]MESA+ Institute for Nanotechnology, University of Twente, P.O. Box 217, 7500 AE Enschede, The Netherlands

[§]Dipartimento di Chimica e Chimica Industriale, Università di Pisa, Via Risorgimento 35, 56126 Pisa, Italy

Supporting Information

ABSTRACT: We investigate here the performance of our recently developed linear-scaling Jastrow-generalized-valence-bond (J-LGVB) wave functions based on localized orbitals, for the quantum Monte Carlo (QMC) calculation of the barrier heights and reaction energies of five prototypical chemical reactions. Using the geometrical parameters from the Minnesota database collection, we consider three hydrogen-exchanges, one heavy-atom exchange, and one association reaction and compare our results with the best available experimental and theoretical data. For the three hydrogen-exchange reactions, we find that the J-LGVB wave functions yield excellent QMC results, with average deviations from the reference values below 0.5 kcal/mol. For the heavy-atom exchange and association reactions, additional resonance structures are important, and we therefore extend our original formulation to include multiple coupling schemes characterized by different sets of localized orbitals. We denote these wave functions as J-MC-LGVB, where MC indicates the multiconfiguration generalization, and show that such a form leads to very accurate barrier heights and reaction energies also for the last two reactions. We can therefore conclude that the J-LGVB theory for constructing QMC wave functions, with its multiconfiguration generalization, is valid for the study of large portions of ground-state potential energy surfaces including, in particular, the region of transition states.

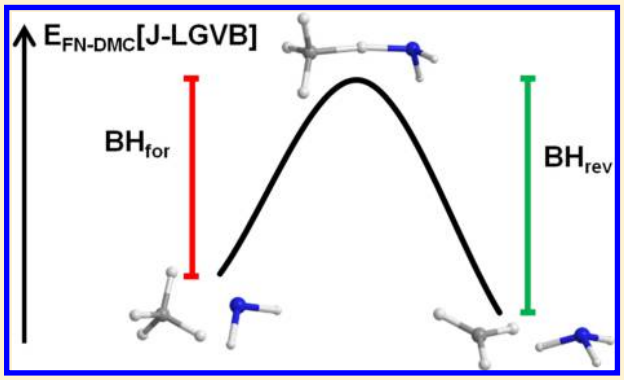

1. INTRODUCTION

We have recently proposed a new class of multideterminantal Jastrow−Slater wave functions to use as trial functions in quantum Monte Carlo (QMC).[1] These wave functions are inspired by the generalized valence bond (GVB) approach and are constructed with localized orbitals (bonding, antibonding, lone-pair, and diffuse lone-pair functions with nodes). The use of localized orbitals allows us to define a coupling scheme between electron pairs, which progressively includes new classes of excitations in the determinantal component of the wave function. The resulting wave functions are rather compact and have a number of determinants that grows linearly with respect to the size of the molecule. We denoted these linear-scaling Jastrow−GVB wave functions as J-LGVBn, where "n" indicates the highest class of excitations included. In our previous work, we demonstrated their excellent performance in the estimate of bond energies of several representative small molecules. Here, we will further test the J-LGVBn wave functions for the calculation of barrier heights of chemical reactions within QMC as well as extend our original formulation to treat multiple resonant configurations (characterized by different sets of localized orbitals), whose inclusion may be needed for an accurate description of the reaction.

While the knowledge of barrier heights is fundamental to understanding the mechanisms of chemical reactions, their correct prediction represents a major challenge for quantum chemical methods since the transition states have usually stretched bonds and are therefore characterized by stronger correlations, often requiring an approach based on a multi-reference wave function. So far, QMC has been applied to the study of barrier heights only in very few cases. We recall (i) the pioneering works of Barnett et al.[2] and Anderson et al.[3,4] on the reaction $H + H_2 \rightarrow H_2 + H$, (ii) the study of the reaction $OH + H_2 \rightarrow H_2O + H$, the decomposition of tetrazine, and the isomerization of vinyl alcohol by Mitas and Grossman,[5] (iii) the dissociation of the H_2 molecule on a silicon surface,[6] and (iv) the dissociation of the tetraoxygen molecule in molecular oxygen.[7] Therefore, this work represents also an opportunity to extend our knowledge on the performance of QMC in the study of chemical reactions as well as to compare the method to other quantum chemical approaches commonly used for this purpose. To this aim, we focus here on three types of processes involving a hydrogen exchange, a heavy atom exchange, and a

Received: May 14, 2013
Published: July 10, 2013

   dx.doi.org/10.1021/ct400395u | J. Chem. Theory Comput. 2013, 9, 3453−3462

reaction of association. All these chemical reactions have been selected from standard databases.

2. METHOD

The general form of the J-LGVBn wave functions is given by

$$\Psi_{\text{trial}} = J\Psi_{\text{LGVBn}} \tag{1}$$

where J is the Jastrow factor and Ψ_{LGVBn} is the determinantal part, which includes up to the n-th class of excitations, as illustrated in more detail in the following. To each order "n" of the LGVB wave function, the number of configuration state functions (CSFs) scales linearly with the size of the system and all valence electrons are correlated. At first order, namely for J-LGVB1, the determinantal part includes only the double excitations from the bonding orbitals to the respective antibonding orbitals for each electron pair as

$$\Psi_{\text{LGVB1}} = c_0|\Phi_0\rangle + \sum_{i=1}^{N/2} c_i|\Phi_{ib\bar{i}\bar{b}}^{ia\bar{i}\bar{a}}\rangle \tag{2}$$

where N is the number of valence electrons in the molecule. In LGVB1, the excitations take into account the correlation only between the electrons within a pair. In the higher orders, further excitations introduce correlations between adjacent pairs of electrons in the molecule. Through the progressive inclusion of new classes of excitations, we obtain 10 LGVBn wave functions of increasing size and accuracy. In LGVB10, the wave function includes all excitations that complete a CAS(4,4) expansion correlating the K adjacent electron pairs of the molecule,

$$\Psi_{\text{LGVB10}} = \sum_{ij}^{K} C_{ij}|\Phi_{ij}\rangle^{\text{CAS(4,4)}} \tag{3}$$

where i and j are the adjacent electron pairs. Here, the number of the CSFs scales linearly with the size of the molecule because the number of the adjacent electron pairs, K, scales also linearly. If a bonding orbital is singly occupied in the reference determinant Φ_0, there will be a CAS(3,4) instead of a CAS(4,4) expansion to describe the coupling between the unpaired electron and a pair of adjacent localized electrons in the above sum. The CSFs included in the two coupling schemes are shown in Tables 1 and 2.

To employ these wave functions in the QMC study of chemical reactions, we must note that the use of localized orbitals, a key feature in the construction of the J-LGVBn wave functions, is also appropriate for the study of transition states. Even though the bonds in these molecular systems can be strongly deformed, a localized description can be maintained in terms of multicentric orbitals. For example, in Figure 1, we show the bonding and antibonding orbitals that describe the three centers-two electrons (3c−2e) N−H−O moiety in the H_2N−H−OH transition state of the reaction, $NH_2 + H_2O \rightarrow NH_3 + OH$.

Finally, while the J-LGVBn wave functions are constructed using one particular resonance scheme, additional resonances may be important for the description of the system of interest. Therefore, we generalize here the functional form of the wave functions to include different coupling schemes, based on different sets of localized orbitals, as

$$\Psi_{\text{trial}} = J\sum_{I} d_I \Psi_{\text{LGVBn}}^{(I)} \tag{4}$$

Table 1. Classes of Excitations (En) that Complete a CAS(4,4) for Two Electron Pairs[a]

code	type	occupation numbers $b_1b_2a_2a_1$
E0	reference	2200
E1	D	0202 + 2020
E2	D	1111
E3	S	1201 + 2110
E4	D	0220 + 2002
E5	Q	0022
E6	T	1021 + 0112
E7	S	1210 + 2101
E8	D	0211 + 2011
E9	D	1120 + 1102
E10	T	1012 + 0121

[a]The excitations with respect to the reference (E0) are labelled as single (S), double (D), triple (T), and quadruple (Q). For the occupation numbers, the order of orbitals is bonding for the pair 1 (b_1), bonding for the pair 2 (b_2), antibonding for the pair 2 (a_2), and antibonding for the pair 1 (a_1). We consider the most common case of a reference (E0) where all the bonding orbitals (or lone pairs functions) are doubly occupied and all antibonding orbitals (or diffuse lone pairs functions with nodes) are empty. For each 2200 coupling, the corresponding CAS(4,4) produces 19 CSFs.

Table 2. Classes of Excitations (En) that Complete a CAS(3,4) for Three Electrons Occupying Two Bonding Orbitals in the Reference (2100)[a]

code	type	occupation numbers $b_1b_2a_2a_1$
E0	reference	2100
E1	D	0102
E2	D	1011
E3	S	1101 + 2010
E4	D	0120
E5	Q	
E6	T	0012
E7	S	1110 + 2001
E8	D	0111
E9	D	1020 + 1002
E10	T	0021

[a]The excitations are labelled as single (S), double (D), triple (T), and quadruple (Q) with respect to the reference (E0). For the occupation numbers, the order of the orbitals is bonding 1 (b_1), bonding 2 (b_2), antibonding 2 (a_2), and antibonding 1 (a_1). For each 2100 coupling, the corresponding CAS(3,4) produces 16 CSFs.

where the summation is over the different configurations, which share the same Jastrow factor but have different orbitals and coefficients of the CSFs. We denote these wave functions as J-MC-LGVBn, where MC indicates a multiconfiguration generalized valence bond wave function.

2.1. Computational Details. In the construction of the Jastrow−Slater J-LGVB1 wave functions, we optimize the orbitals, the coefficients of the CSFs, and the parameters of the Jastrow factor by minimizing the energy at the variational Monte Carlo (VMC) level using the so-called linear method.[8] As initial guess for the orbitals, we take the orbitals obtained from a MCSCF calculation that includes the CSFs of the LGVB1 form and perform the MCSCF calculation using the GAMESS-US package.[9,10] The particular selection of the CSFs included in the LGVB1 wave function ensures that the localization emerges as a result of the variational optimization. For the J-LGVBn ($n > 1$) wave functions, we use the J-LGVB1

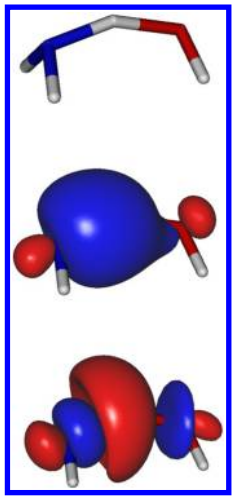

Figure 1. Bonding and antibonding orbitals for the three center two electron N−H−O system in the NH_2H_2O transition state of $NH_2 + H_2O \rightarrow NH_3 + OH$.

orbitals without any further optimization. For the J-MC-LGVBn wave functions, we have additional GVB configurations, characterized by different sets of localized orbitals. The new configurations in the extended MC theory have at least one correlated electron pair in a different region of the molecule, when compared to the main configuration in the original J-LGVBn wave function. In order to construct these new configurations, we have to find a new set of pairs of localized orbitals (the relevant GVB bonding−antibonding orbitals) to accommodate the electron pairs that are in a different region. While chemical intuition through the analysis of the possible resonance structures is a good guide for the definition of the new CSFs in the J-MC-LGVBn wave function, the preparation of the aforementioned additional sets of localized orbitals needs at the moment an *ad hoc* procedure. Since these orbitals are different from those of the most stable GVB configuration, we must force the localization required to describe a new GVB configuration. A possible route is through the deformation of the initial geometry to induce the localization of the electron pairs in selected region of the molecule in combination with standard MCSCF calculations. Once a reliable transformation matrix of atomic orbitals has been obtained, we restore the initial geometry and we switch to the QMC setup to optimize all the orbitals in a J-MC-LGVBn framework. All orbitals of the combined J-MC-LGVB1 wave function are optimized by energy minimization in VMC, together with the Jastrow and CSF parameters. For the J-MC-LGVBn ($n > 1$) wave functions, we use the J-MC-LGVB1 orbitals without any further optimization. The Jastrow factors contain electron−nuclear, electron−electron, and electron−electron-nuclear terms.[11] We employ the Burkatzki et al. (BFD) pseudopotentials[12,13] and the VTZ basis set specifically developed for these pseudopotentials. We also use augmented basis sets, denoted here as aug-VTZ, where we add the diffuse functions of the all-electron aug-cc-pVDZ basis set[14] to the initial BFD VTZ set. The pseudopotentials are treated beyond the locality approximation[15] and a time step of 0.05 au is used in the fixed-node diffusion Monte Carlo (DMC) calculations. All QMC calculations are performed with the CHAMP program.[16] The molecular geometries are taken from the Minnesota Database Collection[17] and were obtained from an optimization at the QCISD/MG3 level of the theory, where MG3[18] is the G3large basis set[19] without the core polarization functions. Finally, the coupled cluster calculations are performed in the frozen-core approximation with the ORCA code.[20,21]

3. RESULTS

In order to assess the performance of the J-LGVBn wave functions in QMC calculation of the barrier heights for chemical reactions, we choose to study five reactions, that is, the following three hydrogen transfers, one heavy atom transfer, and one association reaction:

$$\begin{aligned} &NH_2 + H_2O \rightarrow NH_3 + OH \\ &NH_2 + CH_4 \rightarrow NH_3 + CH_3 \\ &OH + CH_4 \rightarrow H_2O + CH_3 \\ &H + N_2O \rightarrow N_2 + OH \\ &H + N_2 \rightarrow N_2H \end{aligned} \tag{5}$$

The hydrogen-transfer reactions are included in the HTBH38/04 database[22] while the other two reactions are included in the DBH24/08 database.[23] These two databases provide several data for comparison.

3.1. Reference Data. For the reaction energies, here denoted to as ΔE, we use as reference values the experimental Active Thermochemical Tables (ATcT)[24] data corrected for zero-point energy, spin−orbit interaction, and Born−Oppenheimer approximation. ATcT utilizes a redundant and self-consistent thermochemical network from which the optimal thermochemical values are obtained by simultaneous solution in an error-weighted space. For the zero-point energy corrections, we use the estimates determined from anharmonic force fields calculated at the CCSD(T)/cc-pVQZ level[25] when available, and the semiexperimental data[26] otherwise. For spin−orbit interaction and Born−Oppenheimer approximation, we use the correction calculated by Karton et al.[27]

It is instead much more difficult to get reliable reference data for the barrier heights because the thermodynamic data of the transition states are generally not measurable. From experiments, one can obtain the rate constant of the reaction, which does depend on the barrier height but in a manner that is not known. In the literature, the Arrhenius activation energies derived from the rate constants have been often used as references for the barrier heights. However, the Arrhenius activation energy is a macroscopic quantity, it is temperature dependent, and dynamical simulations have shown that these energies and the barrier heights often differ by 2 kcal/mol or more.[28] In order to overcome these problems, Lynch et al.[28] have proposed a recipe to extract from experimental kinetic data a better estimate of the barrier heights. This method combines the experimental data with the results of dynamical simulations using the relation

$$BH_{ref} = BH_{theory} + RT \ln\left[\frac{k_{theory}(T)}{k_{exp}(T)}\right] \tag{6}$$

where BH_{theory} is the barrier height used in the dynamical calculation, k_{theory} is the calculated reaction rate constant at a given temperature T, and k_{exp} is the rate constant determined experimentally at the same temperature. The relation is based on the assumption that the difference between k_{theory} and k_{exp} is

exclusively a consequence of the error in the calculation of the barrier height BH_{theory}.

In order to estimate the reverse barrier heights, one can simply exploit the relation

$$BH_{ref(rev)} = BH_{ref(for)} - \Delta E \quad (7)$$

and use the knowledge on the forward barrier and the reaction energy. Patton et al.,[29] of the same research group, exploit the experimental reaction energies corrected using the MP2/cc-pVDZ zero-point energies scaled by 0.9790. These semi-experimental estimates for the barrier heights have proven to be useful to parametrize new functionals for DFT but still contain several potential sources of error. In order to reduce the inaccuracy in the $BH_{ref(rev)}$ estimate, we prefer to employ the ATcT reaction energies in eq 7. We stress, however, that the references for the barrier heights are not of the same quality as those for the thermodynamical data of the reaction energies.

3.2. $NH_2 + H_2O \rightarrow NH_3 + OH$. The hydrogen transfer $NH_2 + H_2O \rightarrow NH_3 + OH$ reaction is included in the HTBH38/04 database. This reaction plays an important role in atmospheric chemistry.[30] In particular, the reverse reaction is the rate-determining (slow) step in the oxidation of ammonia in the atmosphere.

To establish a reference for the barrier heights, Lynch et al.[28] apply eq 6 to the reverse reaction, $NH_3 + OH \rightarrow NH_2 + H_2O$. To compute the theoretical rate and barrier height for this reaction, they employ a dual-level reaction-path dynamics,[31] where the stationary points are calculated at the QCISD(T)//MP2/aug-cc-pVTZ level and the rest of the reaction path at the semiempirical level. The zero-point energy corrections are calculated with MP2/aug-cc-pVDZ. For the forward-barrier reference, they use eq 7 with the reaction energy obtained from the experimental atomization energies[32,33] and corrected for the zero-point energies. The zero-point corrections are calculated at the MP2/cc-pVDZ level and scaled by 0.9790[29] for OH and NH_2, and estimated from experimental frequencies for H_2O and NH_3.[34] The resulting reaction energy is 9.5 kcal/mol and differs by 0.6 kcal/mol from the ATcT data corrected for the zero-point energies calculated at a higher level of the theory. Therefore, in Table 3, we also report the forward barrier obtained starting from the reverse barrier by Lynch et al. with the use of the more accurate, corrected ATcT reaction energy.

The QMC results for this reaction are given in Table 3. For comparison, we also report the G4 and CCSD(T) values as well as the DFT results obtained with a few representative functionals chosen among the most widely used and studied in relation to the calculation of barrier heights. We find that the DMC reaction energy is in excellent agreement with the experimental reference also when we employ a single-determinant trial wave function and that the use of J-LGVB1 and J-LGVB2 wave functions does not significantly change the single-determinant result. The extension of the basis set with diffuse functions further improves the agreement with the experimental data for all trial functions. The performance of the CCSD(T) method is also very good, while the various DFT functionals yields errors of about 1−2 kcal/mol.

The DMC value for BH_{for} obtained with a single-determinant wave function and the VTZ basis set differs from the best reference by 2.3 kcal/mol. The agreement improves when the J-LGVBn wave functions are used as the errors decrease to 1.7 and 1.8 kcal/mol for J-LGVB1 and J-LGVB2, respectively. The use of diffuse functions lowers the barriers for all types of wave functions and further reduces the discrepancy with the reference value. With the aug-VTZ basis set, the differences become 2.0, 1.6, and 1.3 kcal/mol for single determinant, J-LGVB1, and J-LGVB2 wave functions, respectively. The reverse barriers show a similar behavior: The error in the single-determinant DMC barrier computed with the VTZ basis set is 2.1 kcal/mol, while using the J-LGVB1 and J-LGVB2 wave functions yields an error of 1.5 and 1.6 kcal/mol, respectively. The barriers obtained with the aug-VTZ basis set are slightly improved.

Table 3. Barrier Heights and Reaction Energies (in kcal/mol) for the Reaction $NH_2 + H_2O \rightarrow NH_3 + OH$[a]

method	BH_{for}	BH_{rev}	ΔE	ref
DMC[1 det]/VTZ	15.6	5.3	10.3	this work
DMC[J-LGVB1]/VTZ	15.0	4.7	10.3	this work
DMC[J-LGVB2]/VTZ	15.1	4.8	10.3	this work
DMC[1det]/aug-VTZ	15.3	5.2	10.1	this work
DMC[J-LGVB1]/aug-VTZ	14.9	4.7	10.2	this work
DMC[J-LGVB2]/aug-VTZ	14.6	4.6	10.0	this work
PBE1PBE/MG3S	7.33	−1.84	9.17	17
B3LYP/MG3S	7.16	−2.26	9.42	17
mPW1PW91/MG3S	8.25	−0.93	9.18	17
MPWB1K/MG3S	13.15	5.04	8.12	17
G4//QCISD/MG3	14.79	4.66	10.13	35
W1	13.92	3.54	10.38	36
CCSD(T)/aug-cc-pVTZ	13.82	3.76	10.06	this work
CCSD(T)/aug-cc-pVQZ	14.19	3.86	10.33	this work
ATcT			10.09	24, 25, 27
ref (Lynch et al.)	12.70	3.2	9.5	37
ref (Lynch et al.) +ATcT for ΔE	13.3			

[a]All the calculations are performed at the QCISD/MG3 geometries. ATcT experimental data are corrected for zero-point energy, spin-orbit interaction, and Born−Oppenheimer approximation. The statistical error on the DMC results is 0.1 kcal/mol.

At the DFT level, all functionals give very low values for BH_{for} and negative values for BH_{rev} with the exception of the MPWB1K functional, which was, in fact, developed with the specific purpose of estimating the barrier heights of chemical reactions. The negative values can be understood with the fact that the molecular geometries used to compute the barriers correspond to the critical points obtained at the QCISD/MG3 level of the theory. Finally, the CCSD(T) energies are much closer to the DMC data. For BH_{for}, the difference between the DMC[J-LGVB2]/aug-VTZ and CCSD(T)/aug-cc-pVQZ results is only 0.4 kcal/mol, and for the reverse barrier, BH_{rev}, the difference is 0.7 kcal/mol.

3.3. $NH_2 + CH_4 \rightarrow NH_3 + CH_3$. In Table 4, we show the results obtained for the hydrogen-transfer reaction $NH_2 + CH_4 \rightarrow NH_3 + CH_3$. The ATcT experimental reference is corrected for zero-point energy, spin−orbit interaction, and Born−Oppenheimer approximation. To compute the zero-point energy correction, we use anharmonic force fields calculated at the CCSD(T)/cc-pVQZ level[25] for NH_3 and NH_2, and semiexperimental data for CH_4 and CH_3.[26]

The reference values for the barrier heights by Lynch et al.[37] are based on the same semiexperimental recipe described in the previous section. For the $NH_2 + CH_4 \rightarrow NH_3 + CH_3$ reaction, the theoretical data are taken from dynamical simulations[38] performed on a reaction-path calculated at the UQCISD(T)/6-311+G(2df,2p)//UQCISD/6-311G** level with zero-point corrections evaluated with UQCISD/6-311G** in the harmonic approximation. The reverse barrier is then obtained

dx.doi.org/10.1021/ct400395u | J. Chem. Theory Comput. 2013, 9, 3453−3462

Table 4. Barrier Heights and Reaction Energies (in kcal/mol) for the Reaction $NH_2 + CH_4 \rightarrow NH_3 + CH_3$[a]

method	BH_{for}	BH_{rev}	ΔE	ref
DMC[1det]/VTZ	14.9	17.3	−2.5	this work
DMC[J-LGVB1]/VTZ	14.4	16.8	−2.6	this work
DMC[J-LGVB2]/VTZ	14.6	17.3	−2.8	this work
DMC[1det]/aug-VTZ	14.4	17.1	−2.9	this work
DMC[J-LGVB1]/aug-VTZ	14.4	17.1	−2.9	this work
DMC[J-LGVB2]/aug-VTZ	14.5	17.4	−3.0	this work
PBE1PBE/MG3S	10.02	12.65	−2.63	17
B3LYP/MG3S	11.39	13.49	−2.10	17
mPW1PW91/MG3S	11.02	13.54	−2.52	17
MPWB1K/MG3S	14.32	16.34	−2.02	17
G4//QCISD/MG3	14.62	17.21	−2.59	35
W1	13.92	16.97	−3.05	36
CCSD(T)/aug-cc-pVTZ	14.04	16.19	−2.15	this work
CCSD(T)/aug-cc-pVQZ	14.02	16.69	−2.67	this work
ATcT			−3.12	24, 25, 27, 34
ref (Lynch et al.)	14.50	17.8	−3.3	37
ref (Lynch et al.) +ATcT for ΔE		17.62		

[a]All the calculations are performed at the QCISD/MG3 geometries. The ATcT experimental reaction energy is corrected for zero-point energy, spin-orbit interaction, and Born−Oppenheimer approximation. The statistical error on the DMC results is 0.1 kcal/mol.

through the use of eq 7, where ΔE is computed as the difference between the atomization energy of products and reactants and corrected for the zero-point energies. These corrections are calculated within MP2/cc-pVDZ and scaled by 0.9790[29] for CH_3 and NH_2 and estimated from experimental frequencies for CH_4 and NH_3.[34] The difference between the ATcT reaction energy and the value by Lynch et al. is 0.2 kcal/mol, and in Table 4, we also report the reverse barrier computed with the use of the ATcT reaction energy starting from the forward barrier by Lynch et al.

We find that the DMC reaction energy calculated using the VTZ basis set with the single determinant wave function only differs by 0.6 kcal/mol from the ATcT reference value. With the J-LGVB1 and J-LGVB2 wave functions, the differences are 0.5 and 0.3 kcal/mol, respectively. The use of diffuse functions in the basis set reduces these errors to 0.2 kcal/mol for the single determinant and the J-LGVB1 function and to 0.1 kcal/mol for the J-LGVB2 function, therefore, comparable to the statistical errors on the reaction energies.

Our DMC barrier heights are also in very good agreement with the reference values by Lynch et al. For BH_{for}, the J-LGVB1 and J-LGVB2 barriers are within 0.1 kcal/mol of the reference with both the VTZ and the aug-VTZ basis set. For a single-determinant wave function, we obtain a similar agreement with the use of diffuse basis and a barrier slightly higher by 0.5 kcal/mol when employing a VTZ basis set. For BH_{rev}, the difference between our best DMC J-LGVB2/aug-VTZ result and the reference is only 0.4 kcal/mol, and if we estimate BH_{rev} using the more accurate ATcT value for ΔE in eq 7, the difference is reduced to 0.2 kcal/mol. The CCSD(T) calculations yield lower barriers, which are, however, rather comparable to the DMC values. More precisely, the difference between DMC[J-LGVB2]/aug-VTZ and CCSD(T)/aug-cc-pVQZ is 0.5 kcal/mol for BH_{for} and 0.7 kcal/mol for BH_{rev}. As for the previous reaction, all the density functionals considered in this work underestimate considerably the barriers heights, The only exception is again the MPWB1K functional, which, for this reaction, yields results comparable to our DMC values.

3.4. $OH + CH_4 \rightarrow H_2O + CH_3$. The results obtained for the hydrogen transfer reaction $OH + CH_4 \rightarrow H_2O + CH_3$ are collected in Table 5. In this table, the Lynch et al.[37] reference

Table 5. Barrier Heights and Reaction Energies (in kcal/mol) for the Reaction $OH + CH_4 \rightarrow H_2O + CH_3$[a]

method	BH_{for}	BH_{rev}	ΔE	ref
DMC[1det]/VTZ	7.4	20.0	−12.7	this work
DMC[J-LGVB1]/VTZ	6.9	19.7	−12.8	this work
DMC[J-LGVB2]/VTZ	7.1	20.1	−12.9	this work
DMC[1det]/aug-VTZ	7.1	19.9	−12.9	this work
DMC[J-LGVB1]/aug-VTZ	6.6	19.6	−12.9	this work
DMC[J-LGVB2]/aug-VTZ	6.8	19.7	−12.9	this work
PBE1PBE/MG3S	2.07	13.87	−11.81	17
B3LYP/MG3S	2.34	13.86	−11.52	17
mPW1PW91/MG3S	2.94	14.65	−11.71	17
MPWB1K/MG3S	7.32	17.46	−10.14	17
G4//QCISD/MG3	7.09	19.81	−12.72	35
W1	6.22	19.66	−13.44	36
W4	6.13	19.36	−13.23	41
CCSD(T)/aug-cc-pVTZ	6.40	18.49	−12.20	this work
CCSD(T)/aug-cc-pVQZ	6.29	19.16	−12.99	this work
ATcT			−13.21	24, 25, 27, 34
ref (Lynch et al.)	6.7	19.6	−12.9	37
ref (Lynch et al.) +ATcT for ΔE		19.9		

[a]All the calculations are performed at the QCISD/MG3 geometries. The ATcT experimental value is corrected for zero-point energy, spin-orbit interaction, and Born−Oppenheimer approximation. The statistical error on the DMC results is 0.1 kcal/mol.

data have been obtained with the same recipe discussed for the two previous reactions and with computed and experimental data now taken from refs 39 and 40.

The reaction energy calculated with DMC is in good agreement with the ATcT value. The three wave functions used in this work (single determinant, J-LGVB1, and J-LGVB2) give rather similar results, with deviations ranging between 0.3 and 0.5 kcal/mol also depending on the basis set. Also, for the reaction barriers, the performance of the three wave functions is not too dissimilar, with J-LGVBn leading to forward barriers lower by 0.3−0.5 kcal/mol than the single-determinant values. The agreement with the reference energies by Lynch et al.[37] is very good, in particular for the J-LGVBn wave functions with the aug-VTZ basis set. The agreement of the W1[36] and W4[41] literature data with our DMC barrier heights is instead not as good. In particular, we find that our DMC barriers are higher than the W4 ones even though the deviation is greater than 1 kcal/mol only for BH_{for} when we employ a single-determinant and the VTZ basis set.

The differences between the DMC[J-LGVB2]/aug-VTZ and CCSD(T)/aug-cc-pVQZ results are relatively small, namely 0.5, 0.5, and 0.1 kcal/mol for BH_{for}, BH_{rev}, and ΔE, respectively. Therefore, for all three hydrogen-exchange reactions considered here, the average discrepancy between the barrier heights obtained with these two methods is 0.6 kcal/mol and the maximum one 0.7 kcal/mol. Therefore, for this type of reactions, the performance of CCSD(T) and DMC is very similar. On the other hand, as for the two previous reactions, the calculated DFT barrier heights are substantially lower than

dx.doi.org/10.1021/ct400395u | J. Chem. Theory Comput. 2013, 9, 3453−3462

the best literature references. For the B3LYP and PBE functionals, the disagreement is as large as 5 kcal/mol. The deviation is considerably reduced only for the MPWB1K functional, which, nevertheless, provides poorer results than CCSD(T) and DMC. Furthermore, it should be noted that, even though this functional gives satisfactory estimates of the barrier heights, it provides worse results for the reaction energies than CCSD(T), DMC, and the other DFT functionals considered here.

3.5. $H + N_2O \rightarrow N_2 + OH$. In Table 6, we show the results for the oxygen-transfer reaction, $H + N_2O \rightarrow N_2 + OH$. For this reaction, kinetic data from simulations are not available, so the best reference data for the reaction barriers are from W4.[23] Since an oxygen instead of a hydrogen is being transferred, more electrons are involved in the breaking and forming of chemical bonds, resulting in higher barriers than in the three previous examples.

Table 6. Barrier Heights and Reaction Energies (in kcal/mol) for the Reaction $H + N_2O \rightarrow N_2 + OH$[a]

method	BH_{for}	BH_{rev}	ΔE	ref
DMC[1det]/VTZ	19.5	88.5	−68.9	this work
DMC[J-LGVB1]/VTZ	18.3	87.1	−68.6	this work
DMC[J-LGVB2]/VTZ	19.3	87.2	−67.8	this work
DMC[J-MC-LGVB1]/VTZ	19.1	85.3	−66.1	this work
DMC[1det]/aug-VTZ	19.7	88.7	−68.9	this work
DMC[J-LGVB1]/aug-VTZ	17.4	86.8	−69.2	this work
DMC[J-LGVB2]/aug-VTZ	19.4	87.1	−67.6	this work
PBE1PBE/MG3S	14.44	68.97	−54.53	17
B3LYP/MG3S	11.81	72.92	−61.11	17
mPW1PW91/MG3S	14.65	71.24	−56.59	17
MPWB1K/MG3S	17.80	80.80	−63.00	17
G4//QCISD/MG3	17.10	82.23	−65.13	35
CCSD(T)/aug-cc-pVTZ	18.07	84.81	−66.74	this work
CCSD(T)/aug-cc-pVQZ	18.18	84.12	−65.94	this work
W1	18.14	83.22	−65.08	42
W4	17.13	82.47	−65.34	23
ATcT			−64.86	24, 25, 27, 34

[a]All the calculations are performed at the QCISD/MG3 geometries. The ATcT experimental data are corrected for zero-point energy, spin-orbit interaction, and Born−Oppenheimer approximation. The statistical error on the DMC energies is 0.1 kcal/mol.

The computed DMC reaction energies differ significantly from the ATcT reference. For the single-determinant wave function with either the VTZ or the aug-VTZ basis set, the discrepancy with the experimental value is about 4 kcal/mol. For the J-LGVB1 wave function, the difference becomes 3.7 and 4.3 kcal/mol with the VTZ and the aug-VTZ set, respectively. Only for the J-LGVB2 wave function, we obtain improved results, with a deviation from experimental reaction energy of 2.9 kcal/mol for the VTZ and 2.7 kcal/mol for the aug-VTZ basis set. Therefore, compared to the three previous cases, the disagreement with the experiment is considerably larger in this reaction.

We can understand the reasons behind this inferior performance by analyzing the form of the J-LGVBn wave functions we use here. For the N_2O molecule, the J-LGVBn wave functions use tetrahedral localized orbitals on the terminal oxygen atom. The structure associated with this scheme of localization provides the absolute minimum of energy in the MCSCF optimization for the LGVB1/VTZ wave function. However, an alternative scheme of localization can be thought leading to two configurations in which the localized orbitals on the oxygen atom are placed in a trigonal arrangement, namely, with the three lone pairs described by two sp^2-type and one p orbitals. In order to add more flexibility to the initial J-LGVBn wave functions, we have attempted a multiconfiguration approach by mixing together the three aforementioned configurations as in eq 4. The orbitals on the oxygen for these three configurations are shown in Figure 2. Taking advantage of the fact that QMC can work with nonorthogonal configuration functions, we can achieve in this way a more accurate description of the N_2O molecule. In Table 6, the reaction and barrier energies obtained with this wave function for N_2O are denoted by J-MC-LGVB1, where MC indicates a multiconfiguration valence bond wave function. The reaction energy with the J-MC-LGVB1 wave function considerably improves the agreement with the experimental reference and the discrepancy is now reduced to 1.2 kcal/mol.

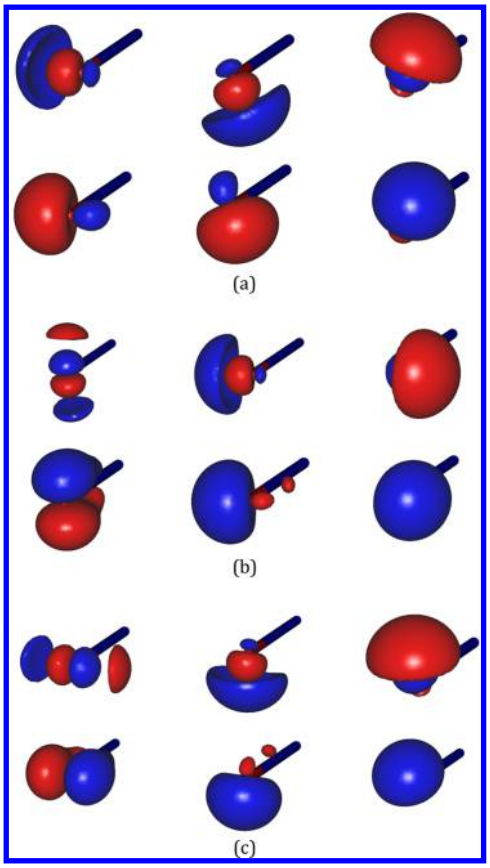

Figure 2. Lone pair orbitals on the oxygen and corresponding diffuse orbitals with nodes in the N_2O molecule. (a) Tetrahedral configuration. (b and c) Trigonal configuration.

In the DMC calculation of the reaction barriers, the use of the single determinant wave function leads to large differences with the W4 data: For the VTZ and aug-VTZ basis sets, the discrepancies are respectively 2.3 and 2.6 kcal/mol in BH_{for}, and 6.0 and 6.3 kcal/mol in BH_{rev}. The use of the J-LGVBn wave functions improves the agreement with the W4 data: with J-LGVB1, the corresponding differences are 1.3 and 0.3 kcal/mol for BH_{for}, and 4.6 and 4.3 kcal/mol for BH_{rev}. For J-LGVB2, the differences become 2.2 and 2.3 kcal/mol in BH_{for}, and 4.7 and 4.3 kcal/mol in BH_{rev}. As for N_2O, also for the transition state,

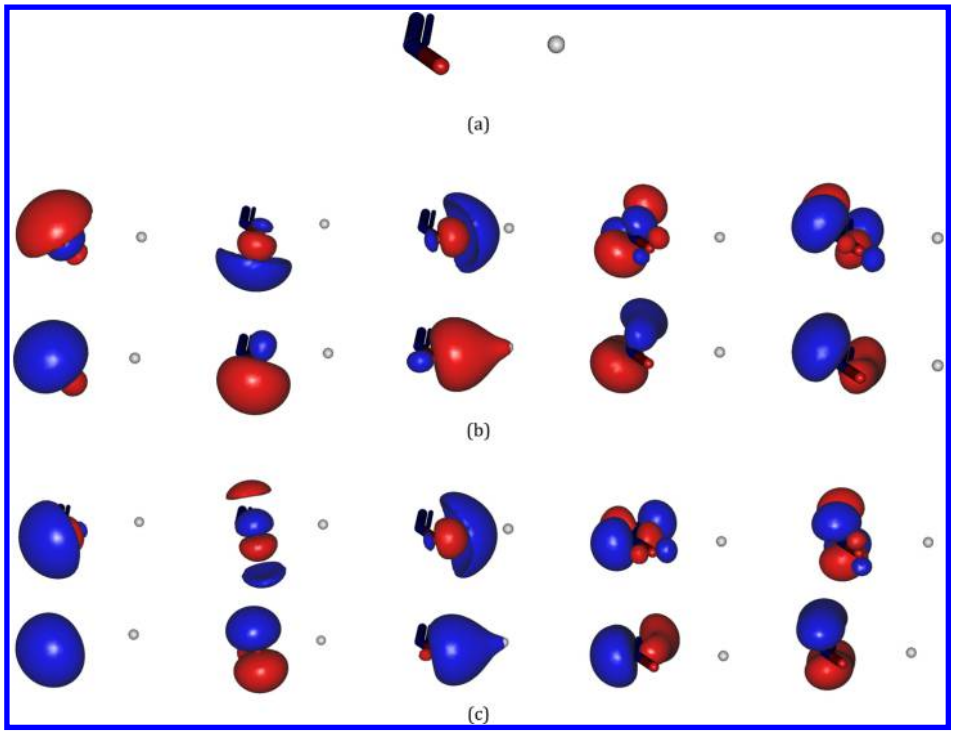

Figure 3. Lone pair and π orbitals on the oxygen for the N_2OH transition state. (a) The molecular structure of the transition state. (b) The configuration with tetrahedral arrangement on the oxygen. (c) The configuration with trigonal arrangement on the oxygen. The different arrangement of the orbitals on the oxygen changes the orientation of the π orbitals between the two nitrogen atoms.

there is a second configuration function coming from a different scheme of localization that can be included to better describe the molecule with localized orbitals. In Figure 3, we show the orbitals of these two different configurations. The orbitals (Figure 3a) belong to the initial J-LGVBn structure, while the orbitals (Figure 3b) are those of the alternative scheme of localization. The use of both configurations in the J-MC-LGVB1/VTZ wave function lowers the discrepancy with the W4 data for BH_{rev} to 2.8 kcal/mol. The error for BH_{for} is instead 1.9 kcal/mol.

For this reaction, the difference between the CCSD(T)/aug-cc-pVQZ and DMC[J-LGVB2]/aug-VTZ results is 1.2 and 3.0 kcal/mol for BH_{for} and BH_{rev}, respectively. The discrepancy is, however, significantly reduced with the use of the J-MC-GVB1/VTZ wave functions, which lead to deviations of 0.9 and 1.2 kcal/mol. Finally, the PBE1PBE, B3LYP, and mPW1PW91 functionals perform very badly in this case, with deviations from W4 for BH_{rev} greater than 10 kcal/mol. MPWB1K gives instead errors smaller than those of our DMC calculations.

3.6. $H + N_2 \rightarrow N_2H$. The association reaction $N_2 + H \rightarrow N_2H$ is included in the DBH24/08[23] database and has also been studied experimentally[43] since it plays an important role in the chemistry of the combustion of nitrogen-containing species. The dissociation of N_2H is exothermic, but there is a barrier of about 10 kcal/mol, which makes this molecule metastable. The N_2H molecule is not contained in the ATcT database, so the best available reference for the reaction energy is the result of the W4 calculation.[23]

For this reaction, in addition to the calculations also performed in all cases studied so far, we carry out a comprehensive study of the J-LGVBn wave functions up to the tenth order with the smaller VTZ basis set. The results are collected in Table 7. For the reaction energy, the one-determinant DMC results differ by 0.7 and 0.6 kcal/mol for the VTZ and aug-VTZ basis sets, respectively. The use of the J-LGVB1 wave functions improves the agreement, lowering these differences to 0.3 and 0.1 kcal/mol, well within the statistical error of 0.1 kcal/mol. Unexpectedly, the results worsen when going from the J-LGVB1 to the J-LGVB2 wave functions. For the J-LGVB2/VTZ wave function, the discrepancy is 1.8 kcal/mol, while for the J-LGVB2/aug-VTZ wave function, the difference is 1.1 kcal/mol. Further increasing the order of the J-LGVBn wave functions does not lead to an improvement: the deviation increases to 3.7 kcal/mol for the J-LGVB4 wave functions and remains substantially constant at all higher orders. To exclude that the disagreement with the best reference is due to the use of pseudopotentials, we perform calculations of ΔE at the CCSD(T) level with the BFD pseudopotentials used in the QMC calculations and report the results in the Table with the CCSD(T)-BFD label. We see that the pseudopotential CC energies agree rather well with the W4 data, in particular, as we increase the size of the basis set used. We can therefore exclude that the discrepancies originate from the use of pseudopotentials.

Clearly, the behavior observed with increasing order of the J-LGVBn wave functions must be explained by considering the resonance structures in detail. The N_2 molecule is well described by a single Lewis structure and, therefore, by a single set of localized orbitals. On the other hand, the N_2H molecule should be described by the three resonance structures shown in Figure 4. We remark that in our calculations we considered only the dominant (Figure 4a) structure. Consequently, we obtain a higher energy for the N_2H molecule and thus overestimate the reaction energy. The very good result obtained with the simplest J-LGVB1 wave function is then due to a favorable cancellation of errors. By performing a J-MC-LGVBn calculation which includes all the three structures of Figure 4, the correct value of reaction energy is achieved at the

dx.doi.org/10.1021/ct400395u | J. Chem. Theory Comput. 2013, 9, 3453−3462

Table 7. Barrier Heights and Reaction Energies (in kcal/mol) for the Reaction $N_2 + H \rightarrow N_2H$[a]

method	BH_{for}	BH_{rev}	ΔE	ref
DMC[1det]/VTZ	15.5	11.0	4.5	this work
DMC[J-FVCAS]/VTZ	13.9	9.3	4.6	this work
DMC[J-LGVB1]/VTZ	15.4	11.3	4.1	this work
DMC[J-LGVB2]/VTZ	15.4	9.8	5.6	this work
DMC[J-LGVB3]/VTZ	15.5	9.6	5.9	this work
DMC[J-LGVB4]/VTZ	16.0	8.6	7.4	this work
DMC[J-LGVB5]/VTZ	16.1	8.7	7.4	this work
DMC[J-LGVB6]/VTZ	16.1	8.6	7.5	this work
DMC[J-LGVB7]/VTZ	16.1	8.8	7.3	this work
DMC[J-LGVB8]/VTZ	16.1	8.9	7.2	this work
DMC[J-LGVB9]/VTZ	16.1	8.9	7.2	this work
DMC[J-LGVB10]/VTZ	16.0	8.7	7.4	this work
DMC[J-MC-LGVB1]/VTZ	13.3	11.2	2.1	this work
DMC[J-MC-LGVB2]/VTZ	13.7	11.2	2.5	this work
DMC[J-MC-LGVB4]/VTZ	14.8	11.0	3.8	this work
DMC[1det]/aug-VTZ	15.5	11.1	4.4	this work
DMC[J-LGVB1]/aug-VTZ	14.3	10.4	3.8	this work
DMC[J-LGVB2]/aug-VTZ	15.1	10.2	4.9	this work
PBE1PBE/MG3S	8.89	11.79	−2.90	17
B3LYP/MG3S	7.82	10.96	−3.14	17
mPW1PW91/MG3S	9.13	11.92	−2.79	17
MPWB1K/MG3S	12.50	13.23	−0.73	17
G4//QCISD/MG3	14.92	10.61	4.31	35
CCSD(T)/aug-cc-pVTZ	14.72	11.00	3.72	this work
CCSD(T)/aug-cc-pVQZ	14.68	10.96	3.72	this work
W1	14.69	10.72	3.97	42
W4	14.36	10.61	3.75	23
CCSD(T)-BFD/VTZ	12.76	9.57	3.19	this work
CCSD(T)-BFD/VQZ	13.68	9.84	3.84	this work
CCSD(T)-BFD/V5Z	13.80	9.86	3.94	this work

[a]All the calculations are performed at the QCISD/MG3 geometries. The statistical error on the DMC results is 0.1 kcal/mol.

fourth order as shown in Table 7 for the VTZ basis set. Therefore, we start from a deviation of 1.7 kcal/mol with the J-MC-LGVB1 wave function and obtain a reaction energy practically equal to the W4 value at the J-MC-LGVB4 level of the theory.

An alternative route to include the effects of resonance is a calculation in which the determinantal expansion is generated by a full valence CAS (FVCAS). We perform here such a calculation for comparison purposes, where we truncate the CASSCF wave function with a threshold over the CSF coefficients chosen to yield 0.997 as the sum of the square of the included coefficients (the complete sum is unity). The resulting J-FVCAS reaction energy is slightly overestimated with respect to the W4 reference but within chemical accuracy.

For the barrier BH_{for} (i.e., for the reaction starting from H + N_2), the single-determinant wave function with the VTZ basis set yields a value 0.8 kcal/mol greater than the W4 reference. The use of the larger aug-VTZ basis set does not change the result. For the reverse barrier, the difference with the W4 reference is 0.4 kcal/mol with the VTZ basis set and 0.5 kcal/mol with aug-VTZ set. Therefore, also for the barrier heights, a single determinant yields a good agreement with the reference values. As for the reaction energy, we perform a comprehensive study of the J-LGVBn trial functions with the VTZ basis set for the barrier height calculation. We find that the different wave functions give two possible values for the BH_{for} energy barrier, namely, 15.4(1) kcal/mol for J-LGVBn for $n \leq 3$ and 16.1(1) kcal/mol for $n > 3$. The transition state, as the N_2H minimum, should be described by the resonance structures shown in Figure 4 while, in our calculation, the J-LGVBn wave functions are constructed with localized orbitals reproducing only the (c) structure. If we look at the N−H distance (1.430 Å in the transition state compared to 1.047 Å in the minimum), it seems that the (c) structure should be more important than the other two. Consequently, the deterioration of the result along the J-LGVBn wave functions sequence is less dramatic than what observed for the calculation of the reaction energy. The relative importance of the multireference description for the transition state and the minimum can be directly appreciated by considering BH_{rev}. The barrier decreases from 11.3 to 8.6 kcal/mol in going from J-LGVB1 to J-LGVB4, and the inclusion of the other excitations in the J-LGVBn sequence does not substantially change the result. At the J-LGVB4 level, we obtain in fact a result, which is 2 kcal/mol lower than the W4 reference, confirming that the use of only one scheme of localization leads to a larger error for the minimum than for the transition state. With the larger aug-VTZ basis set, we perform calculations only for the J-LGVB1 and J-LGVB2 wave functions, and observe a better agreement with the W4 data. The difference between the DMC[J-LGVB2]/aug-VTZ and CCSD(T)/aug-cc-pVQZ results, BH_{for}, is only 0.4 kcal/mol. For the reverse barrier, the difference is 0.8 kcal/mol. Therefore, despite the lack of inclusion of all the resonance structures, the DMC[J-LGVB2]/aug-VTZ is in good agreement with CCSD(T). By including the three structures through the above J-MC-LGVBn wave functions, the agreement for both forward and reverse barriers is better than the J-LGVBn values obtained with the same VTZ basis set. More precisely, the discrepancies with the W4 BH_{for} are, respectively, 1.0, 0.7, and 0.4 kcal/mol for J-MC-LGVB1, J-MC-LGVB2 and, J-MC-LGVB4 while the corresponding differences with the W4 BH_{rev} are 0.6, 0.6, and 0.4 kcal/mol. Therefore, this multiconfiguration approach allows us in this case to achieve chemical accuracy.

The J-FVCAS wave functions lead to similar but slightly worse results on the barrier heigths, the discrepancies with W4 data being 0.4 and 1.3 kcal/mol on the forward and reverse barriers, respectively.

For the DFT functionals considered in this work, we obtain once again poor results. The calculated ΔE are negative, so the DFT results overestimate the stability of the N_2H molecule.

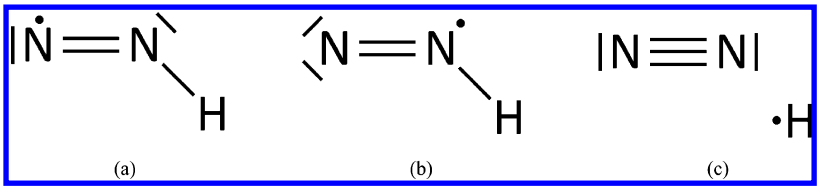

Figure 4. Resonance structures for the minimum and the transition state of the N_2H system.

The BH_{for} energies obtained in DFT are too low, with discrepancies with respect to the W4 values of 1.86, 5.23, 5.47, and 6.54 kcal/mol for the MPWB1K, mPW1PW91, PBE1PBE, and B3LYP functionals, respectively. For BH_{rev}, the agreement with the W4 reference is better.

4. CONCLUSIONS

In this paper, we have tested the performance of J-LGVBn wave functions in the QMC calculation of the barrier heights for five chemical reactions, namely, three hydrogen exchange, one heavy atom exchange, and one association. For the three hydrogen-exchange reactions, the performance of the J-LGVBn functions is excellent. In Table 8, we collect the mean absolute deviations (MAD) for the relative six barriers (forward and reverse) with respect to the most accurate experimental results. We observe that the use of the J-LGVBn wave functions in DMC leads to a small but appreciable improvement compared to the calculations with single-determinant wave functions. The addition of a set of diffuse functions to the basis set further reduces the MAD values by 0.1, 0.1, and 0.3 kcal/mol for the single-determinant, J-LGVB1, and J-LGVB2 wave functions, respectively. DMC[J-LGVB2]/aug-VTZ gives the best performance and compares well with accurate W1 computed values[36] as well as with G4//QCISD/MG3[35] and CCSD(T)/aug-cc-pVQZ (this work). DFT with the functionals selected in this work yields a poor estimate of these barrier heights. Only the MPWB1K functional shows a performance for the barriers comparable with the highly correlated methods above but fails in estimating the reaction energy.

Table 8. Mean Absolute Deviation (MAD, kcal/mol) for the Barrier Heights and the Reaction Energies of the Hydrogen-Exchange Reactions Considered in This Work[a]

method	MAD(BH)	MAD(ΔE)
DMC[1det]/VTZ	1.0	0.4
DMC[J-LGVB1]/VTZ	0.7	0.4
DMC[J-LGVB2]/VTZ	0.8	0.3
DMC[1det]/aug-VTZ	0.9	0.2
DMC[J-LGVB1]/aug-VTZ	0.6	0.2
DMC[J-LGVB2]/aug-VTZ	0.5	0.2
G4//QCISD/MG3	0.7	0.3
W1	0.5	0.2
CCSD(T)/aug-cc-pVTZ	0.7	0.7
CCSD(T)/aug-cc-pVQZ	0.6	0.3
PBE1PBE/MG3S	5.1	0.9
B3LYP/MG3S	4.8	1.1
mPW1PW91/MG3S	4.2	1.0
MPWB1K/MG3S	1.0	2.0

[a]For the barrier heights, we use as reference the values by Lynch et al.[28] (forward) and these same values in combination with the ATcT reaction energies[24,25,27] (reverse). For the reaction energies, we use as reference the ATcT data.

For the heavy atom exchange reaction $H + N_2O \rightarrow N_2 + OH$, we encounter significant difficulties in obtaining QMC results of the same quality as for the hydrogen-exchange reactions. Within QMC, the use of the J-LGVBn wave functions always leads to an improvement compared to the single-determinant wave functions, but the deviation from experiments remains non-negligible, even at DMC[J-LGVB2]/aug-VTZ level. Since the J-LGVBn wave functions are constructed using one resonance scheme while other resonances may be important, we test the addition of different coupling schemes, based on different sets of localized orbitals, to the J-LGVB1/TZV wave functions. As expected, the resulting multiconfiguration J-MC-LGVB1 wave function significantly improves the agreement with the reference data.

Similarly, we encounter a problem related to the resonance of different structures also for the association reaction of a hydrogen atom with the nitrogen molecule. In this case, there appears, however, to be a favorable cancellation of errors in the calculation of the barriers at the DMC[J-LGVB2] level. Nevertheless, the problem is evident in the evaluation of the reaction energy, especially when increasing the order of the J-LGVBn wave functions with $n > 2$. We show that the inclusion of the three structures of Figure 4 in the construction of multiconfiguration J-MC-LGVBn lead to very accurate results on barrier heights and reaction energy at the J-MC-LGVB4/VTZ level.

The results of this work show that our J-LGVBn theory for constructing QMC wave functions is valid for the study of large portions of potential energy surfaces including also the points at the geometry of transition states. In some cases, as in the last two reactions considered in this work, the theory needs an extension to a multiconfiguration approach. As shown here, this can be done maintaining a linear scale with the size of the molecule. We are currently working on the development of a more automated procedure to generate such a multiconfiguration wave function (in particular the starting set of orbitals) than that presented for the two aforementioned examples.

■ ASSOCIATED CONTENT

Ⓢ Supporting Information

Geometries of the considered molecules and the FN-DMC energies. This material is available free of charge via the Internet at http://pubs.acs.org/.

■ AUTHOR INFORMATION

Corresponding Author

*E-mail: francesco.fracchia@unife.it; c.filippi@utwente.nl; amovilli@dcci.unipi.it.

Notes

The authors declare no competing financial interest.

■ ACKNOWLEDGMENTS

This work was carried out under the HPC-EUROPA2 project (Project No. 228398) with the support of the European Commission Capacities Area—Research Infrastructures Initiative. This work is part of a national research project cofunded by the Italian Ministry of Research and University (PRIN 2009).

■ REFERENCES

(1) Fracchia, F.; Filippi, C.; Amovilli, C. *J. Chem. Theory Comput.* **2012**, *8*, 1943−1951.
(2) Barnett, R.; Reynolds, P.; Lester, W., Jr. *J. Chem. Phys.* **1985**, *82*, 2700−2707.
(3) Diedrich, D.; Anderson, J. *Science* **1992**, *258*, 786−788.
(4) Diedrich, D.; Anderson, J. *J. Chem. Phys.* **1994**, *100*, 8089−8095.
(5) Grossman, J.; Mitas, L. *Phys. Rev. Lett.* **1997**, *79*, 4353−4356.
(6) Filippi, C.; Healy, S.; Kratzer, P.; Pehlke, E.; Scheffler, M. *Phys. Rev. Lett.* **2002**, *89*, 166102−166105.
(7) Caffarel, M.; Hernández-Lamoneda, R.; Scemama, A.; Ramírez-Solís, A. *Phys. Rev. Lett.* **2007**, *99*, 153001−153004.

(8) Umrigar, C. J.; Toulouse, J.; Filippi, C.; Sorella, S.; Hennig, R. G. *Phys. Rev. Lett.* **2007**, *98*, 110201−110203.
(9) Schmidt, M. W.; Baldridge, K. K.; Boatz, J. A.; Elbert, S. T.; Gordon, M. S.; Jensen, J. H.; Koseki, S.; Matsunaga, N.; Nguyen, K. A.; Su, S.; Windus, T. L.; Dupuis, M.; Montgomery, J. A. *J. Comput. Chem.* **1993**, *14*, 1347−1363.
(10) Ivanic, J.; Ruedenberg, K. *Theor. Chem. Acc.* **2001**, *106*, 339−351.
(11) Filippi, C.; Umrigar, C. J. *J. Chem. Phys.* **1996**, *105*, 213−226.
(12) Burkatzki, M.; Filippi, C.; Dolg, M. J. *Chem. Phys.* **2007**, *126*, 234105−234112.
(13) For the hydrogen atom, we use a more accurate BFD pseudopotential and basis set. Dolg, M.; Filippi, C., private communication.
(14) Kendall, R.; Dunning, T., Jr.; Harrison, R. *J. Chem. Phys.* **1992**, *96*, 6796−6806.
(15) Casula, M. *Phys. Rev. B* **2006**, *74*, 161102−161105.
(16) CHAMP is a quantum Monte Carlo program package written by Umrigar, C. J.; Filippi, C.; and collaborators.
(17) Minnesota Database Collection, available at http://t1.chem.umn.edu/misc/database_group/database_therm_bh/ (accessed March 9, 2012).
(18) Fast, P. L.; Sánchez, M. L.; Truhlar, D. G. *Chem. Phys. Lett.* **1999**, *306*, 407−410.
(19) Curtiss, L. A.; Raghavachari, K.; Redfern, P. C.; Rassolov, V.; Pople, J. A. *J. Chem. Phys.* **1998**, *109*, 7764−7776.
(20) Neese, F. *ORCA*, An ab initio, Density Functional and Semiempirical program package, Version 2.8.; Max-Planck-Insitut für Bioanorganische Chemie: Mülheim an der Ruhr, 2011.
(21) Neese, F. *WIREs Comput. Mol. Sci.* **2012**, *2*, 73−78.
(22) Zhao, Y.; Lynch, B.; Truhlar, D. *Phys. Chem. Chem. Phys.* **2005**, *7*, 43−52.
(23) Zheng, J.; Zhao, Y.; Truhlar, D. *J. Chem. Theory Comput.* **2009**, *5*, 808−821.
(24) Ruscic, B.; Pinzon, R.; Morton, M.; von Laszevski, G.; Bittner, S.; Nijsure, S.; Amin, K.; Minkoff, M.; Wagner, A. *J. Phys. Chem. A* **2004**, *108*, 9979−9997.
(25) Tajti, A.; Szalay, P.; Császár, A.; Kállay, M.; Gauss, J.; Valeev, E.; Flowers, B.; Vázquez, J.; Stanton, J. *J. Chem. Phys.* **2004**, *121*, 11599−11613.
(26) Karton, A.; Rabinovich, E.; Martin, J.; Ruscic, B. *J. Chem. Phys.* **2006**, *125*, 144108−144124.
(27) Karton, A.; Daon, S.; Martin, J. M. *Chem. Phys. Lett.* **2011**, *510*, 165−178.
(28) Lynch, B.; Patton, L.; Harris, M.; Truhlar, D. *J. Phys. Chem. A* **2000**, *104*, 4811−4815.
(29) Patton, L.; Corchado, J.; Sanchez, M.; Truhlar, D. *J. Phys. Chem. A* **1999**, *103*, 3139−3143.
(30) Diau, E.; Tso, T.; Lee, Y. *J. Phys. Chem.* **1990**, *94*, 5261−5265.
(31) Corchado, J.; Espinosa-Garcia, J.; Hu, W.; Rossi, I.; Truhlar, D. *J. Phys. Chem.* **1995**, *99*, 687−694.
(32) Ruscic, B.; Feller, D.; Dixon, D.; Peterson, K.; Harding, L.; Asher, R.; Wagner, A. *J. Phys. Chem. A* **2001**, *105*, 1−4.
(33) Tratz, C.; Fast, P.; Truhlar, D. *PhysChemComm* **1999**, *2*, 70−79.
(34) Martin, J. *J. Chem. Phys.* **1992**, *97*, 5012−5018.
(35) Curtiss, L.; Redfern, P.; Raghavachari, K. *Chem. Phys. Lett.* **2010**, *499*, 168−172.
(36) Boese, A.; Martin, J. *J. Chem. Phys.* **2004**, *121*, 3405−3416.
(37) Lynch, B.; Truhlar, D. *J. Phys. Chem. A* **2002**, *106*, 842−846.
(38) Yu, Y.; Li, S.; Xu, Z.; Li, Z.; Sun, C. *Chem. Phys. Lett.* **1998**, *296*, 131−136.
(39) Melissas, V. S.; Truhlar, D. G. *J. Chem. Phys.* **1993**, *99*, 3542−3552.
(40) Atkinson, R. *J. Phys. Chem. Ref. Data Monograph* **1989**, *1*, 18−18.
(41) Karton, A.; Tarnopolsky, A.; Lamère, J.; Schatz, G.; Martin, J. *J. Phys. Chem. A* **2008**, *112*, 12868−12886.
(42) Zhao, Y.; González-García, N.; Truhlar, D. *J. Phys. Chem. A* **2005**, *109*, 2012−2018.
(43) Selgren, S.; McLoughlin, P.; Gellene, G. *J. Chem. Phys.* **1989**, *90*, 1624−1629.